

Complex modes in damped sandwich beams using beam and elasticity theories

Naveed Ahmad^{*1} and Rakesh K. Kapania^{2a}

¹Department of Engineering Science and Mechanics, Virginia Tech, Blacksburg, VA, USA

²Department of Aerospace and Ocean Engineering, Virginia Tech, Blacksburg, VA, USA

(Received August 27, 2014, Revised September 30, 2014, Accepted September 30, 2014)

Abstract. We investigated complex damped modes in beams in the presence of a viscoelastic layer sandwiched between two elastic layers. The problem was solved using two approaches, (1) Rayleigh beam theory and analyzed using the Ritz method, and (2) by using 2D plane stress elasticity based finite-element method. The damping in the layers was modeled using the complex modulus. Simply-supported, cantilever, and viscously supported boundary conditions were considered in this study. Simple trigonometric functions were used as admissible functions in the Ritz method. The key idea behind sandwich structure is to increase damping in a beam as affected by the presence of a highly-damped core layer vibrating mainly in shear. Different assumptions are utilized in the literature, to model shear deformation in the core layer. In this manuscript, we used FEM without any kinematic assumptions for the transverse shear in both the core and elastic layers. Moreover, numerical examples were studied, where the base and constraining layers were also damped. The loss factor was calculated by modal strain energy method, and by solving a complex eigenvalue problem. The efficiency of the modal strain energy method was tested for different loss factors in the core layer. Complex mode shapes of the beam were also examined in the study, and a comparison was made between viscoelastically and viscously damped structures. The numerical results were compared with those available in the literature, and the results were found to be satisfactory.

Keywords: finite element method; damping; sandwich beam; complex modes; viscoelasticity; constrained damping treatment; modal strain energy method

1. Introduction

Extensive literature is available on damping of structural vibrations and noise by employing a viscoelastic layer sandwiched between two elastic layers. These types of sandwich structures are frequently used in the aerospace and automotive industry (Rao 2003, Lee 2008), and provide an effective mean of dissipating the noise and vibrational energy by using a soft and heavily damped viscoelastic material. The main idea behind this type of structures is that damping can be obtained due to highly damped shear vibrations in the viscoelastic core layer, sandwiched between two elastic layers. Transverse shear strain is usually not considered in the elastic layers.

*Corresponding author, Ph.D. Student, E-mail: navid@vt.edu

^aMitchell Professor, E-mail: rkapania@vt.edu

Constrained layer damping has an advantage over unconstrained or free layer damping. In the unconstrained damping treatment, the viscoelastic material is subjected to extensional deformation during cyclic deformation, whereas in constrained layer damping, the material is subjected to shear deformation. Sun and Lu (1995) considered that this added advantage of constrained layer is due to the high difference in the moduli of the elastic and core layers. In the category of constrained layer damping, treatments in which the base and the constraining elastic layers have same thickness are considered to provide maximum damping due to high shear deformation (Abdoun *et al.* 2009).

Rao and Nakra (1973) considered the longitudinal and rotary inertias in the core for both plates and beams having constrained layers. But they reported that while these inertias do not play a vital role when we consider homogeneous beams vibrating at low frequencies, these can be of significant importance if interest is in very high frequencies. For unsymmetric beams, these inertias have to be considered even for low frequencies due to inherent coupling between in-plane and transverse vibrations.

Fasana and Marchesiello (2001) used the Rayleigh-Ritz method for constrained layer beams. They followed the work by Rao and Nakra (1973) by including the longitudinal and rotation inertias in the core layer. They used simple polynomials as admissible functions for different boundary conditions. Singhvi and Kapania (1994) reported the limitations of employing simple polynomials over trigonometric and other orthogonal functions. They showed that as the number of terms using simple polynomials is increased; the mass and stiffness matrices become computationally singular especially for higher modes but on the other hand, orthogonal functions do not suffer from such limitations. In view of this, we used trigonometric functions as admissible functions in the Ritz method to obtain the damped response.

Rikards (1993) and Barkanov (1993) used beam elements to calculate the frequency and loss factors. Rikards used four superelements with third-order approximation, each element having 8 nodes and 20 degree of freedom, with same transverse displacement through the thickness of the beam. Barkanov used four elements with 61 degrees of freedom to model a sandwich beam having different materials for the base and constraining layer. Use of higher order finite element helps in better approximation of damping ratios. Imaino and Harrison (1991) showed that by using the p -version finite element method we can get good estimates of damping, especially for sandwich structures with lower core moduli. Johnson and Kienholz (1982) used NASTRAN commercial software for the three dimensional finite element analysis. They used quadrilateral and triangular plate elements for modeling the face layers and a solid element to model the core layer. Kosmatka and Liguore (1993) reported the use of finite element analysis for constrained layer damping, and a comparison between different methods used to calculate the damped response.

Sainsbury and Zhang (1999) used the Galerkin element method for analyzing the damped sandwich beams. Bhimaraddi (1995) used non-linear variation to employ non-uniform shear stress variation through the thickness of the core. He concluded that this theory is suitable for structures having thick core layers. Hu *et al.* (2008) reviewed the classical and higher-order theories to model sandwich structures as well as the Zig-Zag models and concluded that all these theories include shear deformation in the kinematic formulation by using some assumptions. They also reported that higher-order theories take great effort to implement, but does not give better results as compared to the first-order shear deformation theory, in view of 3D elasticity equations. Sanliturk and Koruk (2013) developed a composite finite element with damping capability, employing rotational degrees of freedom.

The Modal strain energy (MSE) method has been extensively used in literature as well as

commercially, to include viscoelastic properties in the finite-element analysis. MSE method was first used by Johnson and Kienholz (1982) to calculate the loss factor from undamped real modes. It is based on the assumption that damped, and undamped mode shapes of the sandwich structure are identical, and the natural frequency predictions of the sandwich structure is independent of the damping level (Koruk and Sanliturk 2012, Sanliturk and Koruk 2013). MSE method has some limitations because of the inherent assumption of similar mode shapes. Method of Complex eigenvalues (MCE) has also been used frequently in the literature. Rikards and Barkanov (1992) used MCE and reported that this method need more computation time as compared to the problem without damping.

Koruk and Sanliturk (2011) reviewed both MSE and MCE methods, and concluded that complex eigenvalue method gives accurate results at the expense of huge CPU time; on the other hand, MSE is computationally efficient but better accuracy is not obtained for highly damped structures, although, the qualitative predictions of MSE are quite acceptable. We will investigate the ability of MSE method to predict the overall loss factor corresponding to different core loss factors, and compare it with MCE and published analytical results. Koruk and Sanliturk (2012) reported that the accuracy of MSE method is strongly dependent on the mean angle of the complex eigenmodes. For mean angle less than 5%, the error in the loss factor prediction by MSE was only 3%. Koruk and Sanliturk (2014) used MSE method, because of its computational efficiency, to optimize general viscoelastically damped structures.

Role of non-proportional damping on the complex mode shapes in structures has been reported in the literature. Koruk and Sanliturk (2013) developed a new complexity factor for general structures based on conservation of energy principle, for quantification of complex modes. They reported that the mode shape complexity in non-proportionally damped structures is generally higher than proportionally damped structures. Therefore, the notion of normal modes cannot be used in the modal analysis for highly non-proportionally damped structures. Koruk and Sanliturk (2014) reported that the accuracy of the MSE method decreases as the mode shape complexity increases in general damped structures. Lampoh, Charpentier, and Mostafa (2014) used homotopy-based asymptotic numerical method, to determine the sensitivity of complex eigenvalue solution in damped sandwich structures to various perturbations. Adhikari (2004) developed a normalization procedure for complex modes, using a least-square error minimization approach.

In the present paper, simple trigonometric functions are used as admissible functions in the Ritz method to obtain the damped response, and the convergence rate of these functions is compared with simple polynomial functions. The principle of virtual work is used along with the Rayleigh beam theory, by including the longitudinal and rotational inertias in the formulation. In most of the work available in the literature, the authors used either different beam theories or finite element with multi degree-of-freedom beam elements. In defining these beam theories and beam elements, different assumptions are made, such as shear is neglected in face layers. In the present paper, an investigation is made on the use of plane stress elasticity based finite element formulation to get improved natural frequencies and loss factor estimates. In this procedure, no kinematic assumptions are considered in the face as well as core layers. All the layers are modeled using 2D elements in the normal direction, and transverse shear strains are introduced in both elastic and core layers. Moreover, an effect on the damped response of the sandwich structure from using 4-noded as well as 9-noded rectangular elements is investigated. The frequency and loss factor is calculated for each mode using both the method of complex eigenvalues and the modal strain energy method. The efficiency of the modal strain energy method is tested for different loss factors in the core layer. Complex mode shapes of the beam are studied in this paper and a comparison is made

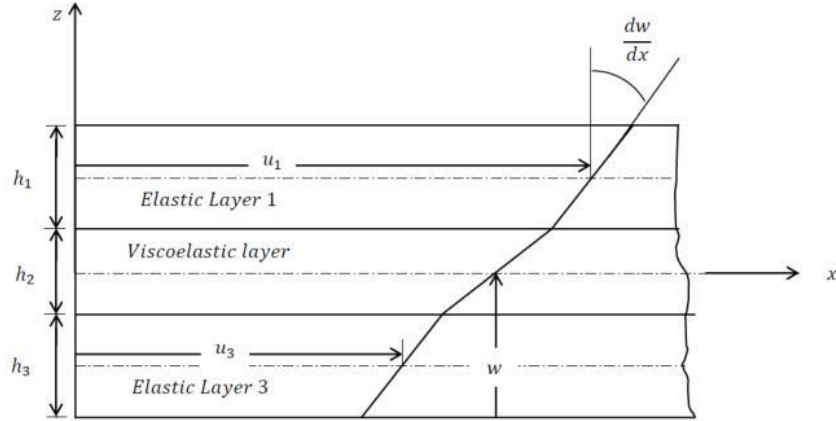


Fig. 1 Schematic of the damped sandwich structure

between viscoelastically and viscously damped structures.

2. Rayleigh-Ritz method

2.1 Strain and kinetic energies

The assumptions made in this study, for the damped structure shown in Fig. 1, are as follows,

1. The face and core layers are assumed to be homogenous and isotropic.
2. Planes perpendicular to the middle plane before bending remains plane after deformation.
3. Normal stresses and extension in the core layer are neglected.
4. All displacements and rotations are considered small.
5. All three layers undergo same deflection.
6. The longitudinal displacements in the layers change linearly through the thickness as shown in Fig. 1.
7. Along the interface, no slip condition and continuity of displacements is considered.

The displacement field for the faces can be written as

$$\text{For Face 1: } u = u_1 - zw' \quad (1)$$

$$\text{For Face 3: } u = u_3 - zw' \quad (2)$$

Where, w is the deflection of the beam and u_1 and u_3 are the longitudinal displacements (at middle surfaces) in layers 1 and 3, respectively. The strain-displacement and constitutive relations for the three layers are as follows (Fasana and Marchesiello 2001)

$$\text{Face 1: } \quad \varepsilon_{xx}^1 = u_1' - zw'' , \quad \sigma_{xx}^1 = E_1 (u_1' - zw'') \quad (3a,b)$$

$$\text{Face 3: } \quad \varepsilon_{xx}^3 = u_3' - zw'' , \quad \sigma_{xx}^3 = E_3 (u_3' - zw'') \quad (4a,b)$$

$$\text{Core: } \gamma_{xz} = \frac{\left(u_1 - \frac{h_1}{2} w'\right) - \left(u_3 + \frac{h_3}{2} w'\right)}{h_2} - w', \quad \tau_{xz} = G_2^* \left[\frac{\left(u_1 - \frac{h_1}{2} w'\right) - \left(u_3 + \frac{h_3}{2} w'\right)}{h_2} - w' \right] \quad (5a,b)$$

Where $()'$ represent the derivative with respect to x -axis, σ and ε are the longitudinal stress and strain in the face layers, τ and γ are the shear stress and strain in the core layer, and E and G are the Young's and shear modulus, respectively. An asterisk denotes a complex quantity throughout this paper; for example $G^* = G(1 + i\eta)$ is the complex shear modulus with η as the loss factor of the core. One can also include the damping in the face layers, which are usually considered elastic, by using complex Young's moduli (Fasana and Marchesiello 2001), as we will see in one of the numerical examples, Example 2.

We can write the virtual work done by the internal stresses as

$$\begin{aligned} \delta W_i &= \int_V (\sigma_{xx}^1 \delta \varepsilon_{xx}^1 + \sigma_{xx}^3 \delta \varepsilon_{xx}^3 + \tau_{xz} \delta \gamma_{xz}) dV \quad (6) \\ \delta W_i &= \int_0^L \{E_1 A_1 u_1' \delta u_1' + E_1 I_1 w'' \delta w'' + E_3 A_3 u_3' \delta u_3' + E_3 I_3 w'' \delta w'' + \frac{G_2^* A_2}{h_2^2} [u_1 \delta u_1 \\ &+ u_3 \delta u_3 - u_1 \delta u_3 - u_3 \delta u_1 + C^2 w' \delta w' + C(u_3 \delta w' + w' \delta u_3 - u_1 \delta w' - w' \delta u_1)]\} dx \quad (7) \end{aligned}$$

Where, $C = (h_1 + h_3)/2 + h_2$, A is the cross sectional area and I is the moment of inertia.

Furthermore, by using d'Alembert's principle, the virtual work due to the inertial forces, including the longitudinal and rotary inertias, can be written as

$$\delta W_{inertial} = \int_0^L \left[\rho_1 \int_{A_1} (\ddot{u}_1 - z\ddot{w}') \delta(u_1 - zw') dA_1 + \rho_3 \int_{A_3} (\ddot{u}_3 - z\ddot{w}') \delta(u_3 - zw') dA_3 + \rho \ddot{w} \delta w \right] dx \quad (8)$$

Where, $\rho = \rho_1 A_1 + \rho_2 A_2 + \rho_3 A_3$ and ρ_1, ρ_2, ρ_3 are the densities of layer 1, 2 and 3, respectively. In the absence of external forces, we can write by using Eqs. (7)-(8), the principle of virtual work as

$$\begin{aligned} &\int_0^L \{E_1 A_1 u_1' \delta u_1' + E_1 I_1 w'' \delta w'' + E_3 A_3 u_3' \delta u_3' + E_3 I_3 w'' \delta w'' + \frac{G_2^* A_2}{h_2^2} [u_1 \delta u_1 + u_3 \delta u_3 - u_1 \delta u_3 \\ &- u_3 \delta u_1 + C^2 w' \delta w' + C(u_3 \delta w' + w' \delta u_3 - u_1 \delta w' - w' \delta u_1)] - \omega^2 [\rho w \delta w + \rho_1 A_1 u_1 \delta u_1 \\ &+ \rho_3 A_3 u_3 \delta u_3 + \frac{w' \delta w'}{12} (\rho_1 A_1 h_1^2 + \rho_3 A_3 h_3^2)]\} dx = 0 \quad (9) \end{aligned}$$

In the above equation, we have assumed the harmonic vibrations of u and w .

2.2 Admissible functions

Now, we can apply Rayleigh-Ritz method to Eq. (9). We can express the displacements as a sum of admissible functions

$$w(x) = \sum_{i=1}^n a_i \phi_i(x), \quad u_1(x) = \sum_{i=1}^n b_i \psi_i(x), \quad u_3(x) = \sum_{i=1}^n c_i \psi_i(x) \quad (10a,b,c)$$

Where 'n' is the number of modes. It should be noted that coefficients, the so-called generalized co-ordinates, \mathbf{a} , \mathbf{b} and \mathbf{c} are arbitrary and independent. Putting these displacement functions in Eq. (9) and separating the coefficients of $\delta \mathbf{a}$, $\delta \mathbf{b}$ and $\delta \mathbf{c}$ and equating them to zero, we can get the following set of equations

$$\begin{aligned} \delta a_j : \quad & \int_0^L \left\{ E_1 I_1 a_i \phi_i'' \delta \phi_j'' + E_3 I_3 a_i \phi_i'' \delta \phi_j'' + \frac{G_2^* A_2}{h_2^2} \left[C^2 a_i \phi_i' \phi_j' + C(c_i \psi_i \phi_j' - b_i \psi_i \phi_j') \right] \right. \\ & \left. - \omega^2 \left[\rho a_i \phi_i \phi_j + \frac{a_i \phi_i' \phi_j'}{12} (\rho_1 A_1 h_1^2 + \rho_3 A_3 h_3^2) \right] \right\} dx = 0 \end{aligned} \quad (11)$$

$$\delta b_j : \quad \int_0^L \left[E_1 A_1 b_i \psi_i' \psi_j' + \frac{G_2^* A_2}{h_2^2} (b_i \psi_i' \psi_j' - c_i \psi_i' \psi_j' - C a_i \phi_i' \psi_j) - \omega^2 \rho_1 A_1 b_i \psi_i \psi_j \right] dx = 0 \quad (12)$$

$$\delta c_j : \quad \int_0^L \left[E_3 A_3 c_i \psi_i' \psi_j' + \frac{G_2^* A_2}{h_2^2} [c_i \psi_i \psi_j - b_i \psi_i \psi_j - C a_i \phi_i' \psi_j] - \omega^2 \rho_3 A_3 c_i \psi_i \psi_j \right] dx = 0 \quad (13)$$

The above equations can be written in the matrix form as

$$\mathbf{K}^* \mathbf{x} = \lambda \mathbf{M} \mathbf{x} \quad (14)$$

Where, $\lambda = \omega^2$ and $\mathbf{x} = [a_i, b_i, c_i]$. The stiffness matrix \mathbf{K} is complex because of the inclusion of complex shear modulus and complex Young's modulus.

We used trigonometric functions as the admissible functions.

For the simply supported case

$$\phi_j(x) = \sin\left(\frac{j\pi x}{L}\right), \quad \psi_j(x) = 1 - \cos\left(\frac{(2j-1)\pi x}{2L}\right), \quad j = 1, 2, 3, \dots, n \quad (15a,b)$$

For the cantilever boundary conditions

$$\phi_j(x) = 1 - \cos\left(\frac{(2j-1)\pi x}{2L}\right), \quad \psi_j(x) = 1 - \cos\left(\frac{(2j-1)\pi x}{2L}\right), \quad j = 1, 2, 3, \dots, n \quad (16a,b)$$

3. Elasticity solution (the plane-stress case)

The governing equations of motion are

$$\frac{\partial \sigma_{xx}}{\partial x} + \frac{\partial \tau_{xz}}{\partial z} = \rho \frac{\partial^2 u}{\partial t^2} \quad (17)$$

$$\frac{\partial \tau_{xz}}{\partial x} + \frac{\partial \sigma_{zz}}{\partial z} = \rho \frac{\partial^2 w}{\partial t^2} \quad (18)$$

Where, u and w are the displacements in the x and z -direction, respectively, as shown in Fig. 2. We assumed that every layer is isotropic, so the stress-strain relation can be written as

$$\begin{Bmatrix} \sigma_{xx} \\ \sigma_{zz} \\ \tau_{xz} \end{Bmatrix} = \begin{bmatrix} C_{11} & C_{12} & 0 \\ C_{12} & C_{22} & 0 \\ 0 & 0 & C_{66} \end{bmatrix} \begin{Bmatrix} \varepsilon_{xx} \\ \varepsilon_{zz} \\ 2\varepsilon_{xz} \end{Bmatrix} \quad (19)$$

The square matrix in the above equation will be complex because of complex shear and Young's moduli for the core layer. This matrix will also be complex for the constraining layers when we will consider complex Young's modulus in the constraining layers.

The strain-displacement relations are given as

$$\varepsilon_{xx} = \frac{\partial u}{\partial x}, \quad \varepsilon_{zz} = \frac{\partial w}{\partial z}, \quad 2\varepsilon_{xz} = \frac{\partial u}{\partial z} + \frac{\partial w}{\partial x} \quad (20a,b,c)$$

By substituting Eqs. (19)-(20) into Eqs. (17)-(18), we obtain the following two equations

$$\frac{\partial}{\partial x} \left(C_{11} \frac{\partial u}{\partial x} + C_{12} \frac{\partial w}{\partial z} \right) + \frac{\partial}{\partial z} \left(C_{66} \frac{\partial u}{\partial z} + C_{66} \frac{\partial w}{\partial x} \right) = \rho \frac{\partial^2 u}{\partial t^2} \quad (21)$$

$$\frac{\partial}{\partial x} \left(C_{66} \frac{\partial u}{\partial z} + C_{66} \frac{\partial w}{\partial x} \right) + \frac{\partial}{\partial z} \left(C_{12} \frac{\partial u}{\partial x} + C_{22} \frac{\partial w}{\partial z} \right) = \rho \frac{\partial^2 w}{\partial t^2} \quad (22)$$

Deriving the weak form and using the test function (Reddy 2005), we obtain

$$\begin{bmatrix} \mathbf{M} & 0 \\ 0 & \mathbf{M} \end{bmatrix} \begin{Bmatrix} \ddot{\mathbf{u}} \\ \ddot{\mathbf{w}} \end{Bmatrix} + \begin{bmatrix} \mathbf{K}^{11} & \mathbf{K}^{12} \\ \mathbf{K}^{21} & \mathbf{K}^{22} \end{bmatrix} \begin{Bmatrix} \mathbf{u} \\ \mathbf{w} \end{Bmatrix} = 0 \quad (23)$$

Where

$$w \approx \sum_{i=1}^n a_i^e \psi_i^e(x, z), \quad u \approx \sum_{i=1}^n b_i^e \psi_i^e(x, z) \quad (24a,b)$$

$$M_{ij} = \int_{\Omega^e} \rho t \psi_i \psi_j dx dz, \quad K_{ij}^{11} = \int_{\Omega^e} t \left(C_{11} \frac{\partial \psi_i}{\partial x} \frac{\partial \psi_j}{\partial x} + C_{66} \frac{\partial \psi_i}{\partial z} \frac{\partial \psi_j}{\partial z} \right) dx dz \quad (25a,b)$$

$$K_{ij}^{12} = K_{ji}^{21} = \int_{\Omega^e} t \left(C_{12} \frac{\partial \psi_i}{\partial x} \frac{\partial \psi_j}{\partial z} + C_{66} \frac{\partial \psi_i}{\partial z} \frac{\partial \psi_j}{\partial x} \right) dx dz \quad (26)$$

$$K_{ij}^{22} = \int_{\Omega^e} t \left(C_{66} \frac{\partial \psi_i}{\partial x} \frac{\partial \psi_j}{\partial x} + C_{22} \frac{\partial \psi_i}{\partial z} \frac{\partial \psi_j}{\partial z} \right) dx dz \quad (27)$$

Where, ψ_i^e are the elemental interpolation functions used in the finite element procedure. The stiffness matrix obtained will be complex in nature. We used bilinear quadrilateral and biquadratic elements along the length and thickness of each layer, respectively.

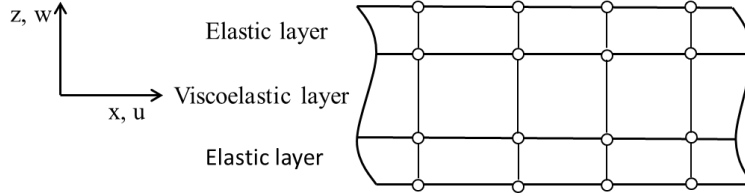


Fig. 2 Schematic of partial sandwich beam with 4-noded elements in face and core layers

4. Frequency and loss factor calculation

After following any of the procedures discussed above, we can come up with a system of equations, which we can write in the matrix form as

$$\mathbf{M}\ddot{\mathbf{x}} + \mathbf{K}^* \mathbf{x} = 0 \quad (28)$$

4.1 Method of complex eigenvalues

By looking at Eq. (28), we see that the stiffness matrix is complex, because of the inclusion of complex shear and Young's moduli. We can solve this equation by using the standard way of solving a real eigenvalue problem, but in this case we will get complex eigenvalues and eigenvectors. Johnson and Kienholz (1981) reported that the complex modes we get are orthogonal in nature and we can get uncoupled equations of motion. They also found that this method costs three times more than the corresponding undamped eigenvalue problem. Kosmatka and Liguore (1993) too found this method to be more accurate but at the same time more computationally expensive because of the complex form of the problem. Method of complex eigenvalues assumes displacements to be harmonic in nature (Rikards 1993) and to be of the form

$$\mathbf{x}^* = \mathbf{x}_0^* e^{i\omega^* t} \quad (29)$$

Where, ω^* is the complex frequency and \mathbf{x}_0^* is complex eigenvector. For free vibration, we can write Eq. (28) as

$$\left(-\lambda^* \mathbf{M} + \mathbf{K}^*\right) \mathbf{x}_0^* = 0 \quad (30)$$

Where, $\lambda^* = (\omega^*)^2$ is the complex eigenvalue. By solving the above system of equations, we get complex eigenvalues and complex frequencies for the damped structure

$$\lambda^* = \lambda + i\lambda' \quad (31)$$

$$\omega^* = \omega + i\omega' \quad (32)$$

The loss factor η_n corresponding to each frequency can be obtained by the following ratio (Rikards 1993)

$$\eta_n = \frac{\lambda'_n}{\lambda_n} \quad (33)$$

Where, λ_n and λ'_n are real and imaginary parts of the complex eigenvalue λ'_n , respectively. It is also possible to calculate the loss factor from the complex frequencies ω^* (Rikards 1993), as follows

$$\eta = 2 \arctan\left(\frac{\omega'}{\omega}\right) \quad (34)$$

Where, ω and ω' are real and imaginary parts of the complex eigenvalue ω^* , respectively.

4.2 The modal strain energy method

Johnson and Kienholz (1981) used this method with NASTRAN commercial engineering software to determine the modal loss factor. The main idea behind this method is that one does not have to solve the complex eigenvalue problem, the loss factor can be found from the undamped real modes. We can use these undamped modes to obtain energy dissipated in the damped structure. Rikards (1993) reported that this method is an approximate method and for small damping the difference between undamped frequencies and modes, and damped frequencies and modes is relatively small. This will save us time and computational cost provided that the modal coupling is negligible (Kosmatka 1993). Moreover, this method assumes that the damping in elastic layers is very small as compared to damping in viscoelastic layer (Johnson and Kienholz 1981). We will use this method only with the plane stress case. Rikards (1993) reported that by using the real undamped modes, we can calculate the energy dissipated (ΔU) in one cycle of steady state vibrations and elastic strain energy (U) using

$$\Delta U = \pi x_{0_n}^T \mathbf{K}' x_{0_n}, \quad U = \frac{1}{2} x_{0_n}^T \mathbf{K} x_{0_n} \quad (35)$$

Where, \mathbf{K} is the real and \mathbf{K}' is the imaginary part of the complex stiffness matrix \mathbf{K}^* and n denotes the n^{th} mode. Now the loss factor can be calculated from the relation (Rikards 1993):

$$\eta_n = \frac{\Delta U}{2\pi U} = \frac{x_{0_n}^T \mathbf{K}' x_{0_n}}{x_{0_n}^T \mathbf{K} x_{0_n}} \quad (36)$$

Table 1 Modal frequencies and loss factors for a simply-supported sandwich beam

	Mode No.	1	2	3	4
Present study ($n = 4$)	ω_n (rad/s)	1206	4638	10345	18318
	η_n (%)	3.57	1.07	0.50	0.28
Present study ($n = 8$)	ω_n (rad/s)	1206	4639	10345	18318
	η_n (%)	3.56	1.07	0.50	0.28
Present study ($n = 12$)	ω_n (rad/s)	1206	4639	10345	18318
	η_n (%)	3.57	1.07	0.50	0.28
Present study ($n = 20$)	ω_n (rad/s)	1206	4639	10345	18318
	η_n (%)	3.56	1.07	0.50	0.28
Fasana and Marchesiello (2001) ($n = 20$)	ω_n (rad/s)	1204	4631	10328	18278
	η_n (%)	3.43	1.07	0.50	0.28

Table 2 Natural frequencies of simply-supported sandwich beam

Mode	Method of complex eigenvalues				Modal strain energy method			
	Ritz method	4 Node	9 Node	Rikards*	4 Node	9 Node	Rikards*	Analytical*
1	904.42	910.75	897.49	1001	850.91	836.00	924	878
2	2488.96	2544.06	2466.83	2723	2491.33	2410.91	2574	2458
3	4948.08	5066.12	4870.07	5256	5015.35	4818.51	4839	4927

*Rikards (1993)

Table 3 Loss factor of simply-supported sandwich beam

Mode	Method of complex eigenvalues				Modal strain energy method			
	Ritz method	4 Node	9 Node	Rikards*	4 Node	9 Node	Rikards*	Analytical*
1	0.57	0.48	0.50	0.38	0.54	0.55	0.45	0.55
2	0.34	0.32	0.34	0.30	0.33	0.35	0.34	0.34
3	0.20	0.20	0.20	0.20	0.20	0.21	0.29	0.20

*Rikards (1993)

5. Results

First, we used the Rayleigh-Ritz method to compare our results with Fasana and Marchesiello (2001) to validate our code. Fasana and Marchesiello also used Rayleigh-Ritz method to solve their problem but they used simple polynomials as admissible functions. We used trigonometric functions and found that we can get a good estimate of lower frequencies and the loss factors with lesser number of modes. Fasana and Marchesiello used 20 modes and we only used 4 modes to get the results with required accuracy as can be seen in Table 1. Of course, we will have to use higher modes for better approximating the higher frequencies. The material and geometric properties used for this beam were; $h_1=0.5$ mm; $h_3=5$ mm; $E_1=E_3=207$ GPa; $\eta_1=\eta_3=0$; $h_2=2.5$ mm; $G_2=4$ MPa; $\eta_2=0.38$; $L=242.5$ mm.

5.1 Example 1: Sandwich beam with pure elastic face

5.1.1 Simply-supported sandwich beam

We modeled simply-supported beam with the same material properties as used by Rikards (1993), namely C2A. The C2A properties are given as $h_1=h_3=3$ mm; $E_1=E_3=45.54$ GPa; $\rho_1=\rho_3=2040$ Kg/m³; $\nu_1=\nu_3=0.33$; $\eta_1=\eta_3=0$; $h_2=3$ mm; $E_2=0.0159$ GPa; $\rho_2=1200$ Kg/m³; $\nu_2=0.45$; $\eta_2=1$; b (width) =15 mm; $L=270$ mm. The face layers are considered completely elastic, i.e., without complex Young's modulus. The core layer is considered viscoelastic with complex shear modulus in which the loss factor (η) does not change with frequency.

We investigated the first three natural frequencies for the simply supported beam using the Rayleigh-Ritz method and using plane stress elasticity with 1200 bilinear quadrilateral (4 node) elements and 300 biquadratic (9 node) elements. Frequency results are shown in Table 2 and the resulting loss factor results are shown in Table 3. We compared our results with Rikards (1993), who used four superelements with third-order approximation, each element having 8 nodes and 20 degree of freedom. Rikards used both method of complex eigenvalues (MCE) as well as the modal strain energy method (MSE) to calculate the frequencies and loss factors. He also reported

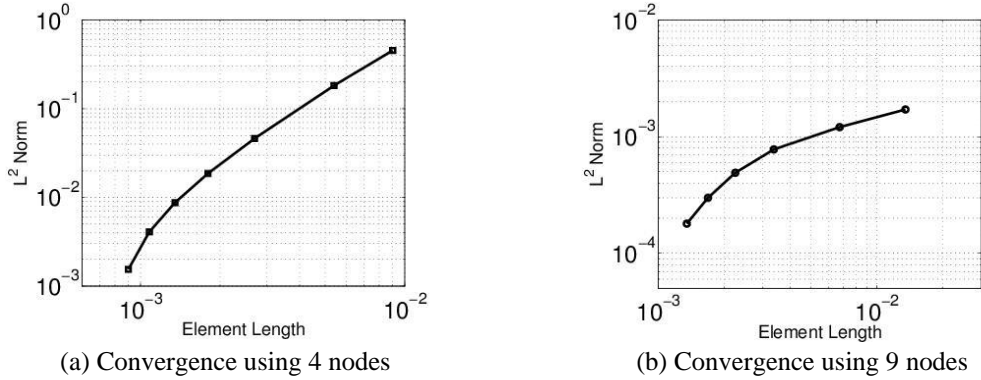


Fig. 3 Convergence plots for sandwich beam with pure elastic faces

Table 4 Natural frequencies for first three modes of cantilever beam with different core loss factors

η_c	Ritz method	MSE	MSE ^a	MCE	MCE ^a	ANM ^b	Analytical ^c
0.1	64.6	64.1	64.1	64.1	64.1	64.2	64.1
	296.7	296.5	296.6	296.6	296.6	296.9	296.4
	744.6	743.8	744.3	743.8	744.4	745.5	743.7
0.6	66.2	64.1	64.1	65.7	65.5	65.6	65.5
	299.9	296.5	296.6	299.8	299.1	299.5	298.9
	747.1	743.8	744.3	746.4	746.2	747.3	745.5
1	68.4	64.1	64.1	67.8	67.4	67.5	67.4
	304.8	296.5	296.6	304.7	303.0	303.3	302.8
	751.6	743.8	744.3	750.8	749.4	750.4	748.6
1.5	71.1	64.1	64.1	70.4	69.9	70.0	69.9
	312.3	296.5	296.6	312.3	309.1	309.4	308.9
	759.8	743.8	744.3	759.0	755.2	756.2	754.0

^aBilasse *et al.* (2010); ^bDaya and Potier-Ferry (2001); ^cSoni (1981)

analytical results based on the sixth order theory derived by Mead and Marcus (1969). Our results are closer to the analytical values reported by Rikards, than those obtained by Rikards himself.

The frequencies predicted by MCE are a bit higher than undamped frequencies but on the other hand the loss factors predicted by MSE are lower than those predicted by MCE. Loss factors obtained using 300 biquadratic elements are higher than using 1200 bilinear quadrilateral elements but for the natural frequencies opposite is the case. Convergence of the first frequency for four and nine node elements is shown in Fig. 3. It is noted that by using a high degree of approximation for the elasticity based FEM, we can get better estimates of the frequencies that are close to the analytical results given by Rikards.

The CPU time for using MCE was 350 seconds as compared to 10 seconds for MSE for the simply supported case. The CPU time was calculated using 1200 quadrilateral elements. The reason for difference in time between the two methods is that we have to solve the entire complex eigenvalue problem in MCE for getting the first three loss factors and frequencies, on the other hand MSE solved for only first three loss factors and we need to solve only the undamped real eigenvalue problem.

Table 5 Loss factor ratio (η_b/η_c) for first three modes of cantilever beam with different core loss factors

η_c	Ritz method	MSE	MSE ^a	MCE	MCE ^a	ANM ^b	Analytical ^c
0.1	0.292	0.283	0.283	0.281	0.281	0.281	0.282
	0.242	0.242	0.243	0.242	0.242	0.242	0.242
	0.154	0.154	0.154	0.154	0.154	0.153	0.154
0.6	0.256	0.283	0.283	0.246	0.246	0.246	0.246
	0.232	0.242	0.243	0.232	0.232	0.232	0.232
	0.153	0.154	0.154	0.152	0.152	0.152	0.153
1	0.212	0.283	0.283	0.202	0.202	0.202	0.202
	0.217	0.242	0.243	0.217	0.217	0.217	0.218
	0.150	0.154	0.154	0.150	0.150	0.150	0.150
1.5	0.162	0.283	0.283	0.153	0.153	0.153	0.153
	0.197	0.242	0.243	0.197	0.197	0.197	0.197
	0.146	0.154	0.154	0.146	0.145	0.145	0.146

^aBilasse *et al.* (2010); ^bDaya and Potier-Ferry (2001); ^cSoni (1981)

5.1.2 Cantilever sandwich beam with different core loss factors

We modeled a cantilever beam with pure elastic face layers with material properties given as $h_1=h_3=1.524$ mm; $E_1=E_3=69$ GPa; $\rho_1=\rho_3=2766$ Kg/m³; $\nu_1=\nu_3=0.3$; $\eta_1=\eta_3=0$; $h_2=0.127$ mm; $E_2=0.001794$ GPa; $\rho_2=968.1$ Kg/m³; $\nu_2=0.3$; b (width)=12.7 mm; $L=177.8$ mm, for various core layer loss factors. We assumed that the complex stiffness is constant and does not change with frequency and thus it leads to a linear complex eigenvalue problem (Bilasse *et al.* 2010). This problem has been extensively studied in the literature (Soni 1981, Daya and Potier-Ferry 2001, Lee 2008, Abdoun *et al.* 2009, Bilasse *et al.* 2010).

We investigated the first three frequencies and the corresponding loss factors (η_b) for the cantilever beam using the Rayleigh-Ritz method with 12 modes and the FEM elasticity method with 300 elements. Natural frequencies (Hz) are reported in Table 4 and the loss factor ratios (η_b/η_c) for the beam are shown in the Table 5 for different core loss factors (η_c).

It is evident from the results that modal strain energy method cannot be used with structures which have a high loss factor as predicted by Johnson and Keinholtz (1981) and reported by Bilasse *et al.* (2010). The MSE approach underestimates the frequencies and overestimates the loss factors for the beams with a high core loss factor. Our results for the MSE were closed to those reported by Bilasse *et al.* (2010). We also compared our results from the plane stress finite element formulation with Daya and Potier-Ferry (2001), who assumed plane strain conditions with 1226 degree of freedom over the beam. The frequency and loss factors estimates were in good agreement. Daya and Potier-Ferry (2001) devised a new numerical method, for solving the nonlinear complex eigenvalue problem, called asymptotic numerical method (ANM) by using a perturbation technique. Our results calculated by using MCE were closed to ANM, because there was no nonlinearity in this example and complex stiffness was considered constant. The results obtained by using method of complex eigenvalues were in good agreement with Soni (1981), who reported the analytical results obtained by using sixth order differential equation.

5.2 Example 2: sandwich beam with damped face layers

We modeled simply supported and cantilever beam, with the following material and geometric properties, as used by Barkanov (1993), $h_1=1.5$ mm; $E_1=69$ GPa; $\rho_1=2760$ Kg/m³; $\nu_1=0.32$; $\eta_1=0.033$; $h_2=0.5$ mm; $E_2=0.00176$ GPa; $\rho_2=980$ Kg/m³; $\nu_2=0.49$; $\eta_2=0.87$; $h_3=4$ mm; $E_3=36$ GPa; $\rho_3=1900$ Kg/m³; $\nu_3=0.28$; $\eta_3=0.004$; b (width)=6 mm; $L=600$ mm. In this example, we considered the elastic layers to have complex Young's modulus. The core layer is considered viscoelastic with complex shear modulus in which the loss factor (η) does not change with frequency.

We investigated the first five frequencies and the corresponding loss factor for both simply supported and cantilever beams using the Rayleigh-Ritz method and the FEM elasticity case. Frequency results are shown in Table 6 and loss factor results are shown in Table 7. We compared our results with Barkanov (1993). Barkanov used four finite elements with 61 degree of freedom for the simply supported beam and ten finite elements with 150 degree of freedom. Barkanov used Lanczos method for solving the complex eigenvalue problem. Frequencies obtained by using the two methods are lower than Barkanov (1993). The loss factor estimates were higher than that of Barkanov for the simply supported boundary conditions and were close to the results obtained for

Table 6 Natural frequencies for sandwich beam with damped face layers

	Method of complex eigenvalues			Energy method		Barkanov*
	Ritz method	4 Node	9 Node	4 Node	9 Node	
Simply-Supported	190.50	191.45	179.51	183.71	171.10	183.40
	562.01	621.00	561.03	611.33	549.75	577.90
	1141.86	1288.30	1140.00	1281.45	1131.77	1170.30
	1942.91	2211.53	1937.36	2206.45	1931.38	1999.90
	2969.66	3391.79	2955.79	3387.02	2950.57	3101.30
Cantilever	73.98	77.26	72.87	74.92	70.38	71.60
	344.49	377.90	344.47	369.05	334.79	335.20
	839.95	942.05	838.92	931.18	826.17	820.80
	1529.71	1740.59	1525.82	1733.20	1516.84	1504.60
	2447.26	2803.87	2438.15	2798.05	2431.04	2415.10

*Barkanov (1993)

Table 7 Loss factor for sandwich beam with damped face layers

	Method of complex eigenvalues			Energy method		Barkanov*
	Ritz method	4 Node	9 Node	4 Node	9 Node	
Simply-Supported	0.394	0.210	0.238	0.254	0.290	0.182
	0.239	0.187	0.226	0.194	0.237	0.188
	0.151	0.120	0.150	0.122	0.152	0.132
	0.100	0.081	0.101	0.082	0.101	0.092
	0.071	0.059	0.072	0.060	0.073	0.067
Cantilever	0.150	0.120	0.140	0.160	0.180	0.147
	0.220	0.190	0.220	0.210	0.240	0.209
	0.180	0.150	0.180	0.160	0.190	0.167
	0.130	0.100	0.130	0.100	0.130	0.111
	0.090	0.070	0.090	0.070	0.090	0.077

*Barkanov (1993)

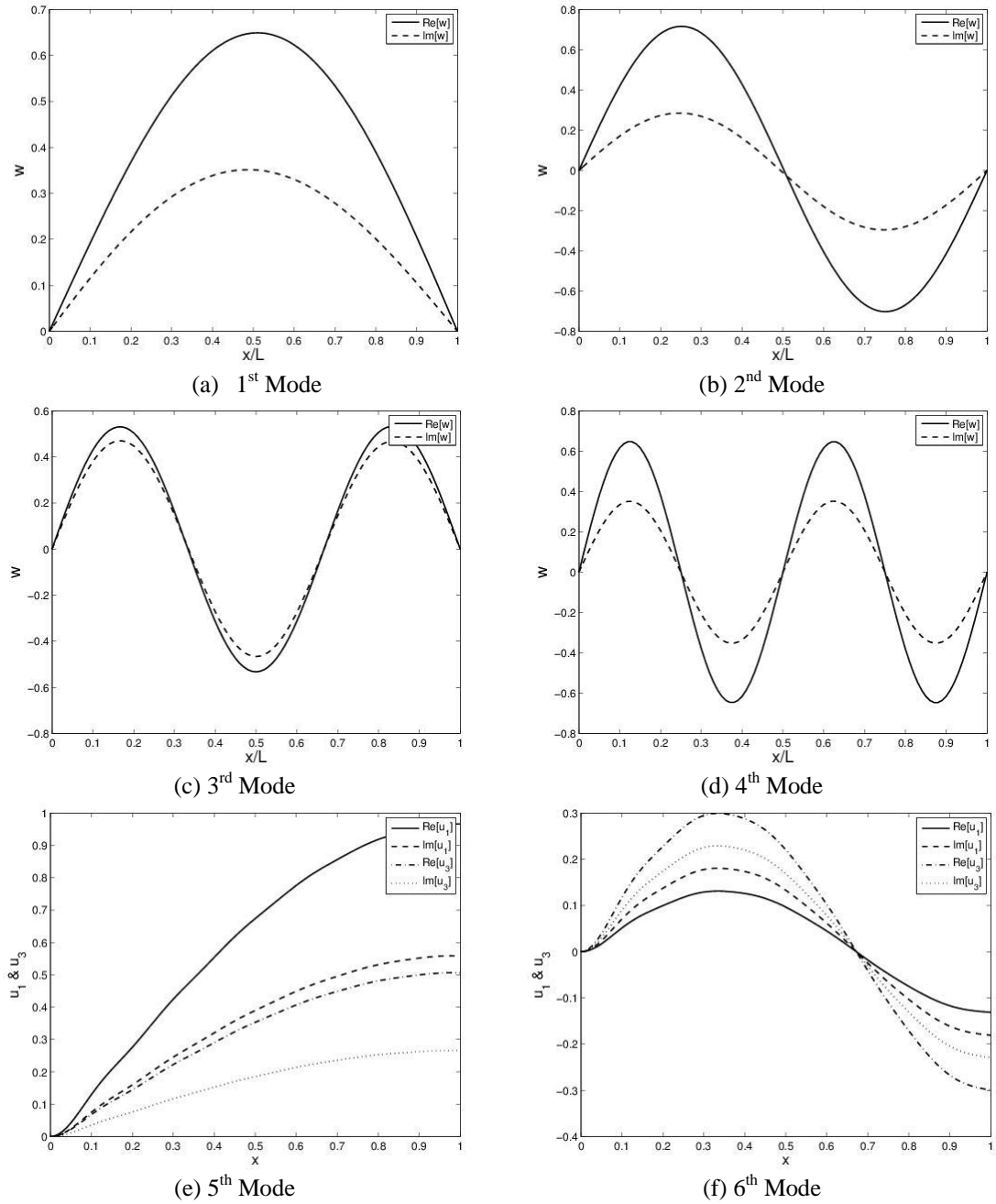


Fig. 4 The real and imaginary parts of mode shapes for S-S sandwich beam with damped face layers

cantilever boundary conditions. It turns out that if we use higher approximation for the elasticity case we can get higher loss factors. The CPU time for using MCE was 763 seconds as compared to 24 seconds for MSE using 1600 quadrilateral elements. First six mode shapes for the simply-supported (S-S) beam using Rayleigh-Ritz method are shown in Fig. 4 with real and imaginary

parts. We note that the real and imaginary parts of the each mode have the same shape but different amplitude as reported by Krenk (2004), Bilasse *et al.* (2010). Moreover, mode shapes for u_1 and u_3 were different because of the different material and thickness used.

5.3 Example 3: investigation of complex mode shapes of a viscoelastically damped sandwich beam with end viscous damper

We investigated the complex mode shapes in detail for the above two examples and the numerical problem considered by Barkanov (1994). We found out that although the eigenvalues and eigenvectors are complex in the case of constrained viscoelastic layer damping, we still get stationary nodes unlike non-proportional viscously damped structures. Prater and Singh (1990) reported that the presence of lumped viscous dampers in the structure move nodes during the cyclic oscillations, and we do not get a single point on the structure where all the displacements go to zero. This lead us to study a cantilever viscoelastic beam with a viscous damper at the free end as shown in Fig. 5, to see how a lumped damper at the boundary can alter the nodal displacements during cyclic oscillations in a damped sandwich beam.

Barkanov (1994) used a damping coefficient value $C=5.00E-04\text{N.s/mm}$ for the end viscous damper, but we noticed that as we increase the value above $5.00E-05\text{N.s/mm}$, the first damped frequency start decreasing and eventually go to zero at $C=5.00E-04\text{N.s/mm}$. This lead us to study a homogeneous beam with an end viscous damper and its equivalent single degree of freedom (SDOF) model included in Appendix. It can be concluded that as we increase damping coefficient (C) above critical damping value, the imaginary part of the complex eigenvalue goes to zero. This implies that the damped natural frequency vanishes at the critical value of C .

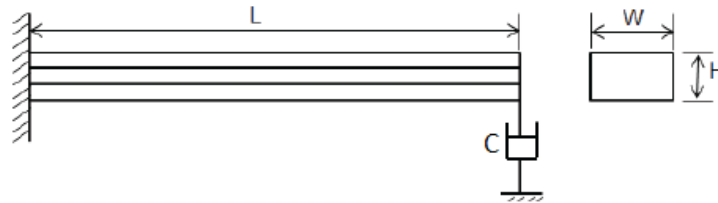


Fig. 5 Schematic of a viscoelastic sandwich beam with end viscous damper

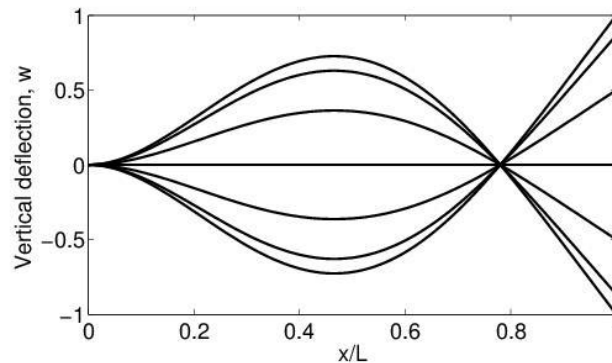


Fig. 6 Displacement of viscoelastic sandwich cantilever beam at different times of cyclic oscillations

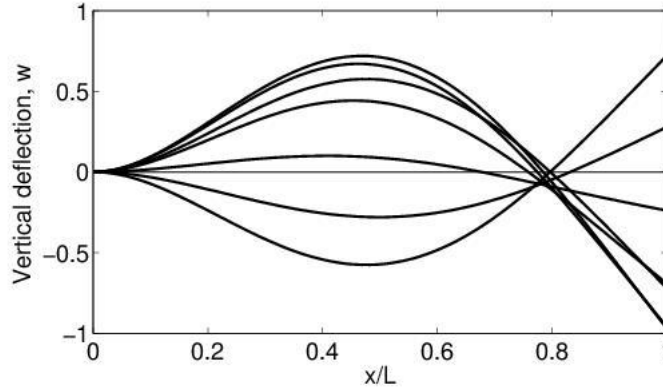


Fig. 7 Displacement of sandwich cantilever beam with end viscous damper at different times of cyclic oscillations, with no material damping $\eta=0$

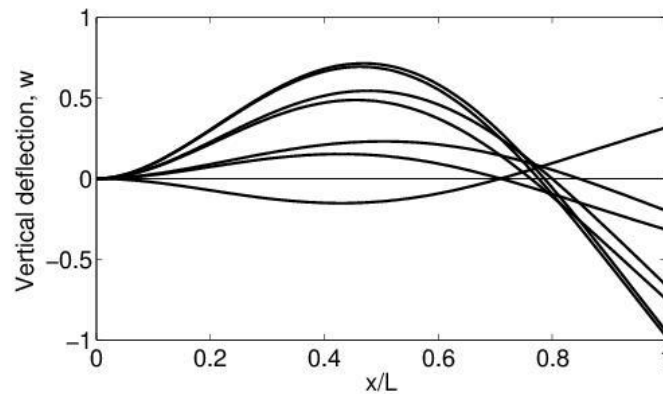


Fig. 8 Displacement of viscoelastic sandwich cantilever beam with end viscous damper at different times of cyclic oscillations

The viscoelastic beam considered by Barkanov (1994) has the following geometric and material properties: $h_1=1.45$ mm; $E_1=127$ GPa; $\rho_1=1900$ Kg/m³; $\eta_1=0.0029$; $h_2=0.127$ mm; $E_2=0.00176$ GPa; $\rho_2=980$ Kg/m³; $\nu_2=0.49$; $\eta_2=0.87$; $h_3=0.254$ mm; $E_3=69$ GPa; $\rho_3=2760$ Kg/m³; $\nu_3=0.32$; $\eta_3=0.033$; W (width)=19.05 mm; $L=203.2$ mm.

We first considered a viscoelastic sandwich beam without a lumped viscous damper. We noticed that we get nodes for each mode, along the length of the beam, for which displacement goes to zero during cyclic oscillations. Figure 6 shows displacements for 2nd mode during one half cycle. Next, we neglected the loss factors in each layer of the cantilever beam and applied a viscous damper at the right end as shown in Fig. 5. We noticed that in this case, we do not get a single point along the beam where all the displacements go to zero during one half cycle as shown in Fig. 7. Moreover, it was noticed that the dispersion of zero displacement points, for higher modes, is wider near the right end of the beam, where viscous damper is mounted. Viscous damping value was considered to be 3.00E-5N.s/mm.

As a last case, we considered viscoelastic damped sandwich beam using both loss factor in each layer and right end viscous damper. As can be seen from Fig. 8, we again do not get stationary

points along the beam and the dispersion of zero displacement points was wider than when only a viscous damper was considered. It was also found that for higher modes this dispersion becomes smaller and we again start seeing stationary nodes along the length of the beam. This can be a good topic for future research in this area.

6. Conclusions

We investigated beams in the presence of a viscoelastic layer sandwiched between two elastic layers. First, the problem was formulated using Rayleigh beam theory and analyzed using Ritz method. We obtained good estimates of natural frequencies and loss factors by using trigonometric functions as compared to using simple polynomials, by using less number of terms in Ritz method. The damping in the layers was modeled using complex modulus. Secondly, the sandwich structure was formulated and analyzed using 2D-plane stress elasticity based finite-element method, without any assumptions for the transverse shear strains. We found that higher degree elements used in the FE elasticity analysis, gives us better estimates of loss factor and natural frequency unlike using beam elements, especially in the problem in which we consider complex stiffness in the elastic layers. The natural frequencies and loss factor were calculated using modal strain energy method and method of complex eigenvalues. MCE gives accurate results but with higher computational cost, especially when a fine mesh is considered. MSE is a cost-effective method but for damping treatments with high loss factors, it overestimates the overall damping of the system.

We observed that although the eigenvalues and eigenvectors are complex in the case of constrained viscoelastic layer damping, we still get stationary nodes unlike non-proportional viscously damped structures. Despite the fact that constrained layer treatment can be quite damped, mode shapes are close to normal modes, and it can be concluded that viscoelastic damping is very close to being proportional. On the other hand, in the case of a viscoelastic damped sandwich beam with end viscous damper, we found that we do not get a single point along the length of the beam where the displacement goes to zero at different times during cyclic oscillations, i.e. the concept of having a node at a point at all times does not exist. Moreover, the mode shapes of the lower modes of a beam with a viscous damper at the free end are more sensitive to the viscous damping coefficient. The complexity of a mode shape is smaller for higher modes of the beam with a viscous damper at the end.

Acknowledgments

N. Ahmad gratefully acknowledges the University of Engineering and Technology (UET) Peshawar, Pakistan for the financial support during his graduate studies.

References

- Abdoun, F., Azrar, L., Daya, E.M. and Potier-Ferry, M. (2009), "Forced harmonic response of viscoelastic structures by an asymptotic numerical method", *Comput. Struct.*, **87**(1), 91-100.
- Adhikari, S. (2004), "Optimal complex modes and an index of damping non-proportionality", *Mech. Syst. Signal Pr.*, **18**(1), 1-27.

- Barkanov, E.N. (1993), "Method of complex eigenvalues for studying the damping properties of sandwich-type structures", *Mech. Comput. Mater.*, **29**(1), 90-94.
- Barkanov, E.N. (1994), "Natural vibrations of a system with hysteretic and viscous damping", *Mech. Comput. Mater.*, **29**(6), 613-616.
- Bhimaraddi, A. (1995), "Sandwich beam theory and the analysis of constrained layer damping", *J. Sound Vib.*, **179**(4), 591-602.
- Bilasse, M., Daya, E.M. and Azrar, L. (2010), "Linear and nonlinear vibrations analysis of viscoelastic sandwich beams", *J. Sound Vib.*, **329**(23), 4950-4969.
- Daya, E.M. and Potier-Ferry, M. (2001), "A numerical method for nonlinear eigenvalue problems application to vibrations of viscoelastic structures", *Comput. Struct.*, **79**(5), 533-541.
- Fasana, A. and Marchesiello, S. (2001), "Rayleigh-Ritz analysis of sandwich beams", *J. Sound Vib.*, **241**(4), 643-652.
- Hu, H., Belouettar, S., Potier-Ferry, M. and Daya, E.M. (2008), "Review and assessment of various theories for modeling sandwich composites", *Comput. Struct.*, **84**(3), 282-292.
- Imaino, W. and Harrison, J.C. (1991), "A comment on constrained layer damping structures with low viscoelastic modulus", *J. Sound Vib.*, **149**(2), 354-359.
- Johnson, C.D. and Kienholz, D.A. (1982), "Finite element prediction of damping in structures with constrained viscoelastic layers", *AIAA J.*, **20**(9), 1284-1290.
- Koruk, H. and Sanliturk, K.Y. (2011), "Assessment of the complex eigenvalue and the modal strain energy methods for damping predictions", *International Congress on Sound and Vibration*, Rio de Janeiro, Brazil, July.
- Koruk, H. and Sanliturk, K.Y. (2012), "Assessment of modal strain energy method: advantages and limitations", *ASME 11th Biennial Conference on Engineering Systems Design and Analysis*, Nantes, France, July.
- Koruk, H. and Sanliturk, K.Y. (2013), "A novel definition for quantification of mode shape complexity", *J. Sound Vib.*, **332**(14), 3390-3403.
- Koruk, H. and Sanliturk, K.Y. (2014), "Optimization of damping treatments based on big bang-big crunch and modal strain energy methods", *J. Sound Vib.*, **333**(5), 1319-1330.
- Kosmatka, J.B. and Liguore, S.L. (1993), "Review of methods for analyzing constrained-layer damped structures", *J. Aerosp. Eng.*, **6**(3), 268-283.
- Krenk, S. (2004), "Complex modes and frequencies in damped structural vibrations", *J. Sound Vib.*, **270**(4), 981-996.
- Lampoh, K., Charpentier, I. and El Mostafa, D. (2014), "Eigenmode sensitivity of damped sandwich structures", *Comptes Rendus Mécanique*, **342**(12), 700-705.
- Lee, D.H. (2008), "Optimal placement of constrained-layer damping for reduction of interior noise", *AIAA J.*, **46**(1), 75-83.
- Mead, D.J. and Markus, S. (1969), "The forced vibration of a three-layer, damped sandwich beam with arbitrary boundary conditions", *J. Sound Vib.*, **10**(2), 163-175.
- Prater, Jr, G. and Singh, R. (1990), "Eigenproblem formulation, solution and interpretation for non-proportionally damped continuous beams", *J. Sound Vib.*, **143**(1), 125-142.
- Rao, Y.V.K.S. and Nakra, B.C. (1973), "Theory of vibratory bending of unsymmetrical sandwich plates", *Arch. Mech.*, **25**, 213-225.
- Rao, M.D. (2003), "Recent applications of viscoelastic damping for noise control in automobiles and commercial airplanes", *J. Sound Vib.*, **262**(3), 457-474.
- Reddy, J.N. (2005), *An Introduction to the Finite Element method*, 3rd Edition, McGraw-Hill, New York, NY, USA.
- Rikards, R.B. and Barkanov, E.N. (1992), "Determination of the dynamic characteristics of vibration-absorbing coatings by the finite-element method", *Mech. Compos. Mater.*, **27**(5), 529-535.
- Rikards, R. (1993), "Finite element analysis of vibration and damping of laminated composites", *Comput. Struct.*, **24**(3), 193-204.
- Sanliturk, K.Y. and Koruk, H. (2013), "Development and validation of a composite finite element with

- damping capability”, *Comput. Struct.*, **97**, 136-146.
- Sainsbury, M.G. and Zhang, Q.J. (1999), “The Galerkin element method applied to the vibration of damped sandwich beams”, *Comput. Struct.*, **71**(3), 239-256.
- Singhvi, S. and Kapania, R.K. (1994), “Comparison of simple and Chebychev polynomials in Rayleigh-Ritz analysis”, *J. Eng. Mech.*, **120**(10), 2126-2135.
- Soni, M.L. (1981), “Finite element analysis of viscoelastically damped sandwich structures”, *Shock Vib. Bull.*, **55**(1), 97-109.
- Sun, C.T. and Lu, Y.P. (1995), *Vibration Damping of Structural Elements*, Prentice Hall Inc., New Jersey, NJ, USA.

EC

Appendix: First eigenvalue of a cantilever beam with end viscous damper

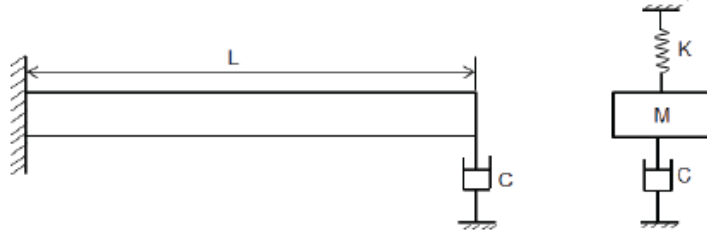


Fig. 9 Schematic of a homogeneous cantilever beam with end viscous damper and its equivalent SDOF model

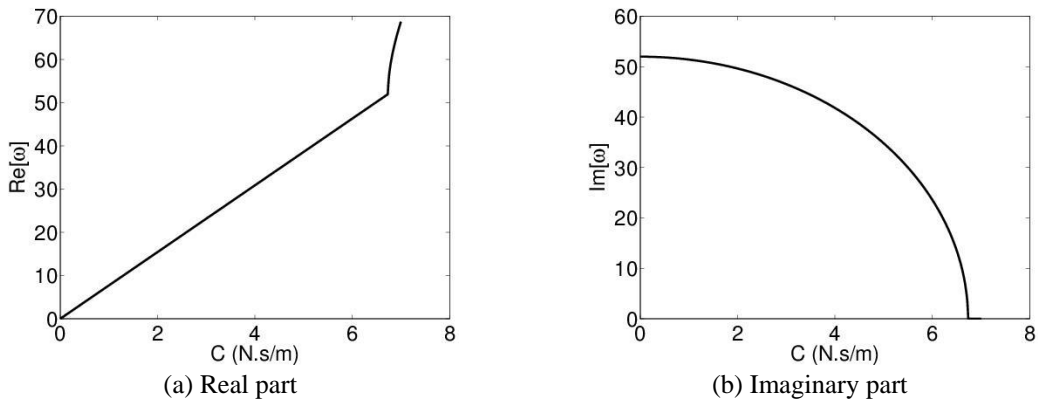


Fig. 10 The real and imaginary parts of the first eigenvalue

A homogeneous aluminum beam as shown in Fig. 9 was considered with 1m length and 0.01m width. The value of damping coefficient C was increased from $1.00E-05$ to $7N.s/m$. The real and the imaginary part of the first eigenvalue are shown in Fig. 10. As the value of C is increased, the imaginary part which is the damped natural frequency gradually goes to zero, and the real part grows. In order to investigate this more, we considered an equivalent SDOF model of the cantilever beam with end viscous damper as shown in Fig. 9. The equivalent stiffness and mass considered are shown below. It was noticed that the imaginary part goes to zero as soon as the value of C approaches the critical value of 6.735.

$$\text{Equivalent Stiffness: } K_{eq} = 3EI / L^3$$

$$\text{Equivalent mass: } m_{eq} = 0.2357 \quad \text{Critical damping: } C_c = 2m_{eq}K_{eq}$$